A new boson approach for the wobbling motion in even-odd nuclei

A. A. Raduta[a),b)], C. M. Raduta [a)] and R. Poenaru [a),c)]
[a)] *Department of Theoretical Physics, Institute of Physics and Nuclear Engineering, Bucharest, POBox MG6, Romania*
[b)] *Academy of Romanian Scientists, 54 Splaiul Independentei, Bucharest 050094, Romania and*
[c)] *Doctoral School of Physics, Bucharest University,*
405 Atomistilor Str., Bucharest-Magurele, Romania

A triaxial core rotating around the middle axis, i.e. 2-axis, is cranked around the 1-axis, due to the coupling of an odd proton from a high j orbital. Using the Bargmann representation of a new and complex boson expansion of the angular momentum components, the eigenvalue equation of the model Hamiltonian acquires a Schrödinger form with a fully separated kinetic energy. From a critical angular momentum, the potential energy term exhibits three minima, two of them being degenerate. Spectra of the deepest wells reflects a chiral-like structure. Energies corresponding to the deepest and local minima respectively, are analytically expressed within a harmonic approximation. Based on a classical analysis, a phase diagram is constructed. It is also shown that the transverse wobbling mode is unstable. The wobbling frequencies corresponding to the deepest minimum are used to quantitatively describe the wobbling properties in ^{135}Pr. Both energies and e.m. transition probabilities are realistically described.

I. INTRODUCTION

The wobbling motion consists in a precession of the total angular momentum of a triaxial system combined with an oscillation of its projection on the quantization axis around a steady position. Bohr and Mottelson described the wobbling motion within a triaxial rotor model for high spin states, where the total angular momentum almost aligns to the principal axis with the largest moment of inertia [1]. This pioneering paper was followed by a fully microscopic description due to Marshalek [2]. Since then, a large volume of experimental and theoretical results has been accumulated [3–22, 24–27]. Also, the concept of wobbling motion has been extended to even-odd nuclei. Experimentally, the excited wobbling states in triaxial super-deformed (TSD) bands are known in several even-odd nuclei like ^{161,163,165,167}Lu, ^{167}Ta [17, 18], ^{135}Pr [28–34], ^{187}Au [34], ^{130}Ba[35] and ^{105}Pd [36].

With the time several formalisms were attempted to describe the wobbling motion in nuclei. Thus, the classical interpretation of Bohr and Mottelson was widely used by various authors in the context of interpreting the new data that meanwhile appeared [5, 9, 30, 35, 37]. The oldest and simplest boson description of the wobbling phenomenon belongs to Bohr and Mottelson [1]. More elaborate interpretations are those of Refs. [14, 15, 23], where Holstein-Primakoff [38] and Dyson [39] boson expansions were used, respectively. The semi-classical studies [16, 24–27, 32] proved to be an efficient and flexible tool for a realistic view of this phenomenon in even-odd nuclei.

The wobbling states are actually fingerprints of the triaxial structure of the nuclei, which justifies the attractive appeal of the subject. The first paper devoted to triaxial nuclei was that of Davydov and Fillipov [42]. The γ deformation of the atomic nuclei has been treated by many authors [43–47]. In Ref.[48], Davydov introduced, for the first time in the literature, a Hamiltonian appropriate for an even-odd nucleus consisting in a core and an odd particle moving in a potential coupling it to the collective core. This Hamiltonian is nowadays widely used by theoreticians. The first results reported for even-odd nuclei within a quasiparticle plus triaxial rotor framework, for the rare earth region, were given in Refs. [49–53].

The wobbling motion has a longitudinal/transversal character depending on whether the relative position of the odd-particle and the core angular momenta are parallel/perpendicular. Although the concept of transverse wobbling is being used by many authors, a certain debate on whether such a wobbling motion exists or not is still standing [27, 29, 31, 37].

In the present paper we propose a new formalism based on a new boson expansion of the angular momentum components. A particular case of the new expansion is a generalization of the Dyson boson representation. By using the Bargmann representation [40], the eigenvalue equation for the model Hamiltonian is brought to a Schrödinger form which, in the harmonic approximation, leads to an explicit expression for the wobbling frequency. Also, a semi-classical description is provided, which is fully consistent with the quantal treatment. Within this picture, it is proved that the transversal mode is unstable despite the fact that we assumed that the middle axis is of maximal MoI. The formalism is applied, with positive result, to ^{135}Pr.

The project sketched above is accomplished according to the following plan. Using a new boson expansion for the angular momentum, in section II the Schrödinger equation for the model Hamiltonian is derived, while in section IV, another boson expansion is obtained. The harmonic approximation is delivered in Section V, while the classical approach is presented in Section VI. In Section VII we give the analytical formulas for the electromagnetic transition probabilities. Numerical results and discussions are presented in Section VIII, while the summary and the final conclusions are described in section IX.

II. A COMPACT FORMULA FOR THE POTENTIAL ENERGY OF A PARTICLE-TRIAXIAL ROTOR HAMILTONIAN

Assuming a rigid coupling of an odd nucleon to a triaxial core, the Hamiltonian for the even-odd system may be approximated as:

$$\hat{H}_{rot} = \sum_{k=1,2,3} A_k (\hat{I}_k - \hat{j}_k)^2, \tag{2.1}$$

with $A_k = \frac{1}{2\mathcal{J}_k}$ and I standing for the total angular momentum.

For a rigid coupling of the odd proton to the triaxial core, we suppose that **j** stays in the principal plane (1,2). Also, we consider that the maximal moment of inertia (MoI) is $\mathcal{J}_2$; furthermore, we expand the linear term in the first order of approximation:

$$\hat{I}_2 = I\left(1 - \frac{1}{2}\frac{\hat{I}_1^2 + \hat{I}_3^2}{I^2}\right). \tag{2.2}$$

Thus, the Hamiltonian acquires the form:

$$\hat{H}_{rot} = A\hat{H}' + (A_1 I^2 - A_2 j_2 I) + \sum_{k=1,2} A_k \hat{j}_k^2, \tag{2.3}$$

where the following notations have been used:

$$\begin{aligned} A &= A_2(1 - \frac{j_2}{I}) - A_1, \\ \hat{H}' &= \hat{I}_2^2 + u\hat{I}_3^2 + 2v_0\hat{I}_1, \ \text{with} \\ u &= \frac{A_3 - A_1}{A}, \ v_0 = \frac{-A_1 j_1}{A}. \end{aligned} \tag{2.4}$$

For what follows, we suppose that the MoI's are such that $1 > u > 0$.

A Hamiltonian similar to $\hat{H}'$, but describing an even-even nucleus, was studied in both semi-classical and quantal frameworks. Here we focus our attention on the quantal description. Note that $\hat{H}'$ looks like a Hamiltonian for a triaxial rotor amended with a term, which cranks the system to rotate around the one-axis. It is convenient to choose the cranking axis as quantization axis. Moreover, it is useful to express the considered Hamiltonian in terms of the raising and lowering angular momenta operators:

$$\hat{I}_\pm = \hat{I}_2 \pm i\hat{I}_3, \ \ \hat{I}_0 = \hat{I}_1. \tag{2.5}$$

In the intrinsic frame of reference, the angular momentum components satisfy the commutation relations:

$$\left[\hat{I}_-, \hat{I}_+\right] = 2\hat{I}_0, \ \ \left[\hat{I}_\mp, \hat{I}_0\right] = \mp\hat{I}_\mp. \tag{2.6}$$

In terms of the new variables, one obtains:

$$\hat{H}' = \frac{1-u}{4}\left(\hat{I}_+^2 + \hat{I}_-^2\right) + \frac{1+u}{4}\left(\hat{I}_+\hat{I}_- + \hat{I}_-\hat{I}_+\right) + 2v_0\hat{I}_0. \tag{2.7}$$

The Schrödinger equation associated to $\hat{H}'$,

$$\hat{H}'|\Psi\rangle = E|\Psi\rangle, \tag{2.8}$$

is further written in terms of the conjugate variables q and $\frac{d}{dq}$, by using the following representation for the angular momentum components:

$$\begin{aligned} \hat{I}_\mp &= i\frac{c \pm d}{k's}\left(I \mp \hat{I}_0\right), \\ \hat{I}_0 &= Icd - s\frac{d}{dq} \equiv \hat{I}_1, \end{aligned} \tag{2.9}$$

where s, c and d denote the Jacobi elliptic functions:

$$\begin{aligned} s &= sn(q,k), \ \ c = cn(q,k), \ \ d = dn(q,k), \ \ \text{with} \\ k &= \sqrt{u}, \ \ k' = \sqrt{1-k^2}, \\ q &= \int_0^\varphi \left(1 - k^2\sin^2(t)\right)^{-1/2} dt \equiv F(\varphi, k). \end{aligned} \tag{2.10}$$

The dependence of the Jacobi functions on the variable q is shown in Fig.1. Their connection with the trigonometric function is given by:

$$s = \sin\varphi, \ \ c = \cos\varphi, \ \ d = \sqrt{1 - k^2 s^2}. \tag{2.11}$$

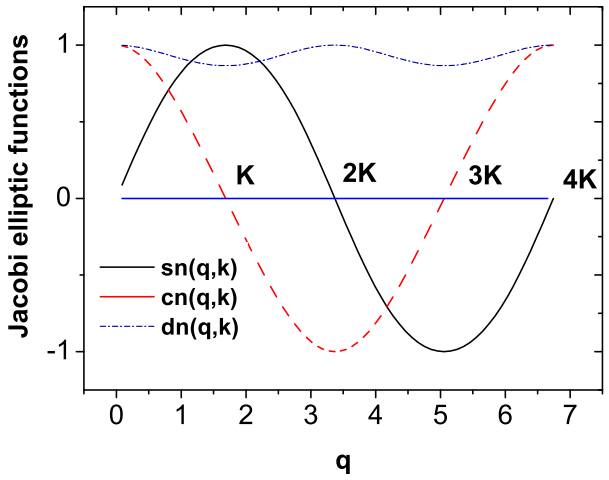

FIG. 1: (Color online) The elliptic functions sn, cn, and dn are represented as function of q, for $k = 1/2$.

Obviously, the functions s, c and d are periodic in φ, with the periods $4K, 4K$ and $2K$ respectively, where:

$$K = F(\frac{1}{2}, k) = \frac{\pi}{2}{}_2F_1(\frac{1}{2}, \frac{1}{2}, 1; k^2). \tag{2.12}$$

The standard notation for the hyper-geometric function ${}_2F_1(\alpha, \beta, \gamma; \epsilon)$, has been used. The magnitude K is

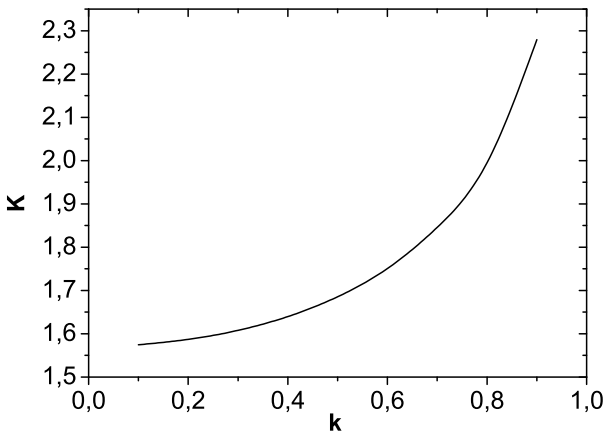

FIG. 2: (Color online) The period K given by Eq.2.12 is plotted as function of k.

plotted as function of k in Fig.2. In terms of the newly introduced conjugate coordinates, $\hat{H}'$ becomes:

$$\hat{H}' = -\frac{d^2}{dq^2} - 2v_0 s\frac{d}{dq} + I(I+1)s^2k^2 + 2v_0 cdI. \quad (2.13)$$

Changing the wave-function by the transformation:

$$|\Psi\rangle = (d - kc)^{-\frac{v_0}{k}}|\Phi\rangle, \quad (2.14)$$

the Schrödinger equation acquires a new form, where the kinetic and potential energies are separated:

$$\left[-\frac{d^2}{dq^2} + V(q)\right]|\Phi\rangle = E|\Phi\rangle. \quad (2.15)$$

The potential energy term has the expression:

$$V(q) = \left[I(I+1)k^2 + v_0^2\right]s^2 + (2I+1)v_0 cd. \quad (2.16)$$

It is worth mentioning that the transformation (2.9) preserves the commutation relations obeyed by the angular momentum components (2.6).

The shape of the potential energy term is shown in Fig. 3. Note that V(q) is invariant with respect to the transformation $q \to -q$. This leads to the fact that in the interval, for example of [-4K,4K], the potential exhibits two deep symmetric wells with degenerate minima, and three local minima in $q = 0, \pm 4K$. States inside the local minima are meta-stable since they are tunnelling to the adjacent deep minima. The states in the deepest wells are degenerate. The shape of the potential V(q) in the interval of [0,4K] is shown in Fig.3, for a few angular momenta I. To visualize the symmetry mentioned above, we plotted V(q) in a larger interval, namely [-4K,4K]. Denoting by ψ_+ the wave function of a state in the right deepest well, and by ψ_- the function corresponding to the same energy as the former state, but the left deepest

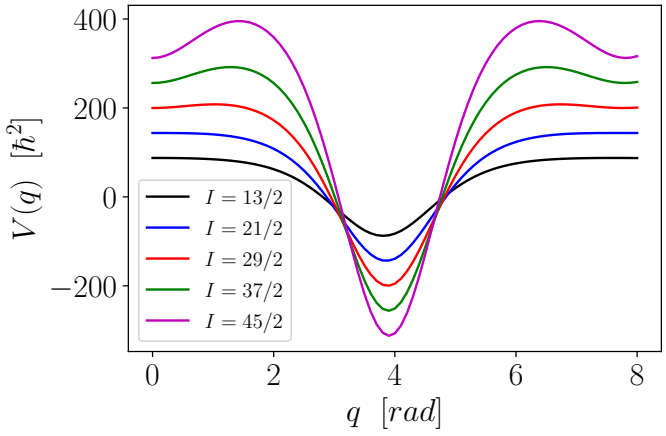

FIG. 3: (Color online) The potential energy is plotted as function of q for a particular set values for the moment of inertia $(MoI) : \mathcal{J}_2 : \mathcal{J}_3 : \mathcal{J}_2 = 100 : 40 : 20\hbar^2 MeV^{-1}$,the odd particle angular momentum j=13/2 and $\theta = \pi/6$.

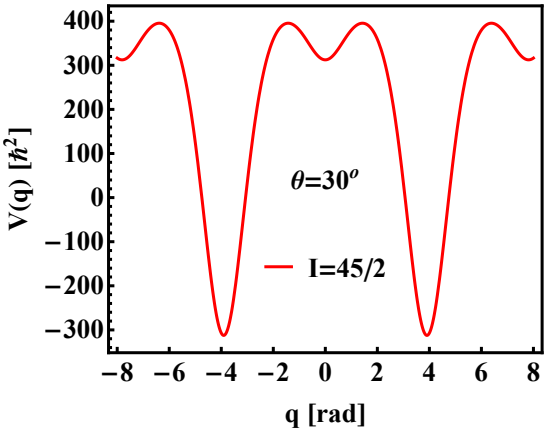

FIG. 4: (Color online) The potential energy is plotted as function of q for a particular set values for the moment of inertia $(MoI) : \mathcal{J}_2 : \mathcal{J}_3 : \mathcal{J}_1 = 100 : 40 : 20\hbar^2 MeV^{-1}$ and $\theta = \pi/6$. Negative values for q are also included. The total angular momentum is I=45/2 and j=13/2.

minimum, they are both spread over the whole interval of [-4K,+4K]. However, the sum $\psi_+ + \psi_-$ is mainly located in the right deepest well, while the difference $\psi_+ - \psi_-$ is mainly spread inside the left deepest well.

In order to prove that the transformation (2.9) preserves the commutation relations for the angular momentum components, we need the first derivatives of the Jacobi functions:

$$\begin{aligned}
\frac{d}{dq}sn(q) &= cn(q)dn(q), \\
\frac{d}{dq}cn(q) &= -sn(q)dn(q), \\
\frac{d}{dq}dn(q) &= -k^2 sn(q)cn(q). \quad (2.17)
\end{aligned}$$

Note now that by using the Bargmann [40] mapping to

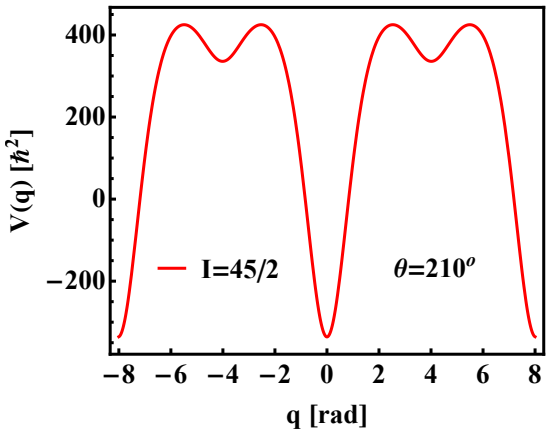

FIG. 5: (Color online) The potential energy is plotted as function of q for a particular set values for the moment of inertia (MoI) : $\mathcal{J}_2 : \mathcal{J}_3 : \mathcal{J}_1 = 100 : 40 : 20\hbar^2 MeV^{-1}$, and $\theta = 7\pi/6$. Negative values for q are also included. The total angular momentum is I=45/2 and j=13/2.

the boson operators $b, b^\dagger$

$$q \to b^\dagger, \quad \frac{d}{dq} \to b, \tag{2.18}$$

it becomes manifest that Eq. (2.9) expresses a homeomorph mapping of the angular momentum components, i.e. the generators of a SU(2) algebra, onto a boson realization of the mentioned algebra. Indeed, within the Bargmann representation we have:

$$\begin{aligned}
\hat{I}_+ &= i\frac{c(b^\dagger) - d(b^\dagger)}{k' s(b^\dagger)} \left(I + Ic(b^\dagger)d(b^\dagger) - s(b^\dagger)b\right), \\
\hat{I}_- &= i\frac{c(b^\dagger) + d(b^\dagger)}{k' s(b^\dagger)} \left(I - Ic(b^\dagger)d(b^\dagger) + s(b^\dagger)b\right), \\
\hat{I}_0 &= Ic(b^\dagger)d(b^\dagger) - s(b^\dagger)b.
\end{aligned} \tag{2.19}$$

To our knowledge this is the first time when such a boson "expansion" shows up in the literature. Obviously, this is different from the known boson expansions proposed by Holstein-Primakoff [38], and Dyson [39]. We note that like the Dyson's, this boson representation does not preserve the hermiticity. Indeed, one can easily check that:

$$\left(\hat{I}_+\right)^+ \neq \hat{I}_- \tag{2.20}$$

Also the boson Hamiltonian, obtained from (2.13) by using he transformation (2.18), is not Hermitic. However, it may be shown [54] that it has real eigenvalues. For our further purposes it is convenient not to use the boson Hamiltonian, but rather the Schrödinger equation (2.15). We remark that, in order to make the Holstein-Primakoff boson expansion tractable, the involved square root operators must be expanded in power series of $\hat{N}/I$, with $\hat{N}$ denoting the boson number operator, while I is the total angular momentum. This expansion is truncated in the second order, and moreover no contribution caused by the normal ordering of the higher order terms, is included. One remarks the fact that the whole boson series involves higher order terms in the linear momentum, which conflicts the semi-classical framework. By contradistinction, in the present case the boson Hamiltonian associated to $\hat{H}'$ is written in a normal order, and is quadratic in the linear momentum $-i\frac{d}{dq}$.

III. ANOTHER NEW BOSON EXPANSION FOR THE A.M. COMPONENTS

The case of $k = 0$ deserves a special attention. Indeed, for this value of k, one obtains:

$$q = \varphi; \quad , d = 1; \quad K = \frac{\pi}{2}, \quad k' = 1. \tag{3.1}$$

Using these simple relations in connection with Eq.(2.19), one obtains a new boson expansion for the angular momentum components in the intrinsic frame:

$$\begin{aligned}
I_+ &= i\left[-I\sin b^\dagger + (1 - \cos b^\dagger)b\right], \\
I_- &= i\left[I\sin b^\dagger + (1 + \cos b^\dagger)b\right], \\
I_0 &= I\cos b^\dagger - \left(\sin b^\dagger\right) b.
\end{aligned} \tag{3.2}$$

Again, this boson expansion is a particular case of Eq.(2.19), and different from the traditional ones mentioned above, as due to Holstein-Primakoff and Dyson. Expanding, consistently, the trigonometric functions, and keeping only the leading terms, we obtain:

$$\begin{aligned}
I_+ &= i\left[-Ib^\dagger + \frac{1}{2}(b^\dagger)^2 b\right], \\
I_- &= 2ib, \\
I_0 &= I - b^\dagger b,
\end{aligned} \tag{3.3}$$

which is just the Dyson boson expansion of the angular momentum components. Due to this result, we may assert that the boson expansions given by Eqs.(2.19), and (3.2) respectively, represent two distinct generalizations of the well known Dyson boson expansion.

IV. HARMONIC APPROXIMATION

Eq.(2.15) can be numerically solved. However, as we shall further see, there are arguments for the validity of the harmonic approximation. First, we look for the stationary point of the potential energy term. These are obtained by looking for the roots of the first derivative of $V(q)$:

$$\begin{aligned}
V'(q) &= s\left[\left(I(I+1)k^2 + v_0^2\right) 2cd - (2I+1)v_0 k'^2\right. \\
&- \left.(2I+1)v_0 2k^2 c^2\right].
\end{aligned} \tag{4.1}$$

Among the stationary points there are five minima for $q = 0, \pm 2K, \pm 4K$, respectively. As shown in Fig. 3, the minima $q = 0$, and $q = \pm 4K$ show up only for $I > 21/2$. The three minima are flat at the beginning, but their depth increases with the spin. The deepest minimum is reached at $q = \pm 2K$. Expanding the potential $V(q)$ up to the second order, in the deviation $q' = q - 2K$, one obtains the equation of a harmonic oscillator, with the spectrum:

$$E'_n = -\frac{(2I+1)^2}{2}v + \sqrt{(1+v)(u+v)(2I+1)^2 - u}\left(n + \frac{1}{2}\right), \tag{4.2}$$

where the notation $v = 2v_0/(2I+1)$ was used.

We recall now that the true Hamiltonian is $\hat{H}_{rot}$, related with $\hat{H}'$ through Eq.(2.4). Thus, the final spectrum has the expression:

$$E_n = A_1 I^2 + (2I+1)A_1 j_1 - I A_2 j_2 + \hbar\omega(n+1/2) + \sum_{i=1,2} A_i {j_i}^2. \tag{4.3}$$

where the frequency ω is defined by:

$$\begin{aligned} \omega &= \left[\left((2I+1)(A_2 - A_1 - \frac{A_2 j_2}{I}) - 2A_1 j_1\right)\right. \\ &\times \left((2I+1)(A_3 - A_1) - 2A_1 j_1\right) \\ &- \left.(A_3 - A_1)(A_2 - A_1 - \frac{A_2 j_2}{I})\right]^{1/2}. \end{aligned} \tag{4.4}$$

Following the same procedure as before, we may expand the potential around the local minimum, $q = 0$, if that exists, and keep only up to the quadratic term, we obtain the following quantal energies:

$$E_n = A_1 I^2 - (2I+1)A_1 j_1 - I A_2 j_2 + \hbar\omega'(n+1/2) + \sum_{i=1,2} A_i {j_i}^2, \tag{4.5}$$

where the new frequency has the expression:

$$\begin{aligned} \omega' &= \left[\left((2I+1)(A_2 - A_1 - \frac{A_2 j_2}{I}) + 2A_1 j_1\right)\right. \\ &\times \left((2I+1)(A_3 - A_1) + 2A_1 j_1\right) \\ &- \left.(A_3 - A_1)(A_2 - A_1 - \frac{A_2 j_2}{I})\right]^{1/2}. \end{aligned} \tag{4.6}$$

Of course, the phonon energies depend on the angle θ defining the components j_1, and j_2 of the single particle angular momentum. It is worth remarking that while the phonon energy ω defined inside the deepest well is a decreasing function, the energy of the phonon defined in the local minimum has an opposite behavior (see Fig. 6).

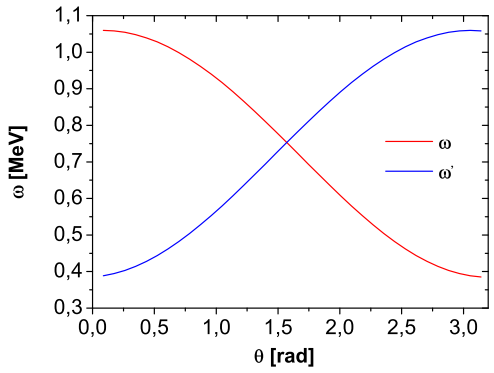

FIG. 6: (Color online) The phonon energies ω and ω' are plotted as function of θ defining the orientation of **j** in the plane XOY. for the moments of inertia (MoI) : $\mathcal{J}_1 : \mathcal{J}_3 : \mathcal{J}_2 = 100 : 40 : 10\hbar^2 MeV^{-1}$.

V. CLASSICAL DESCRIPTION

The classical picture is obtained by the diagonalization procedure, which consists in replacing the operators $\hat{I}_k$ with the classical component of the angular momentum,I_k and the algebra multiplication by:

$$[,] \to -i\{,\}, \tag{5.1}$$

with the notation $\{,\}$ for the Poisson bracket. Let us now denote by φ_k the conjugate coordinate of I_k. Thus, the classical counterpart of the Hamiltonian $\hat{H}'$ is:

$$H' = I_2^2 + uI_3^2 + 2v_0 I_1, \tag{5.2}$$

and one easily finds that:

$$\{I_k, H'\} = \dot{I}_k, \tag{5.3}$$

which leads to the following equations of motion:

$$\begin{aligned} \dot{x}_1 &= 2(1-u)x_2 x_3, \\ \dot{x}_2 &= 2(x_1 u - v_0)x_3, \\ \dot{x}_3 &= -2(x_1 - v_0)x_2, \end{aligned} \tag{5.4}$$

where, for simplicity, the notation $x_k = I_k$, k=1,2,3 has been used. Also, the symbol " $\bullet$ " is used for the time first derivative. Using the equations of motion (5.4), one proves that there are two constants of motion:

$$\begin{aligned} E &= x_2^2 + ux_3^2 + 2v_0 x_1, \\ I^2 &= x_1^2 + x_2^2 + x_3^2. \end{aligned} \tag{5.5}$$

This is a reflection of the fact that the energy, and the angular momentum are conserved. The above equation allows us to express x_2, and x_3 in terms of x_1. Making the time derivative of the first equation (5.4), and inserting the expressions of x_2, and x_3 in the resulting equation, one obtains the final equation for x_1:

$$\ddot{x}_1 + a_3 x_1^3 + a_2 x_1^2 + a_1 x_1 + a_0 = 0, \tag{5.6}$$

where the coefficients have the expressions:

$$\begin{aligned} a_3 &= 8u, \\ a_2 &= -12v_0(1+u), \\ a_1 &= 16v_0^2 - 8uI^2 + 4E(1+u), \\ a_0 &= -8v_0E + 4v_0(1+u)I^2. \end{aligned} \tag{5.7}$$

We recognize in (5.6) the differential equation for the elliptic functions of the first kind. Their explicit expressions can be obtained from the equations of motion (5.4). Indeed, from (5.5) one obtains:

$$\begin{aligned} x_2 &= (1-u)^{-1/2}\left(ux_1^2 - 2v_0x_1 + E - uI^2\right)^{1/2}, \\ x_3 &= (1-u)^{-1/2}\left(-x_1^2 + 2v_0x_1 - E + I^2\right)^{1/2}, \end{aligned} \tag{5.8}$$

and then the first equation (5.4) can be integrated with the result:

$$\begin{aligned} t - t_0 &= \int_{x_{10}}^{x_1} \frac{dx}{2\sqrt{-u(x-\alpha_1)(x-\alpha_2)(x-\alpha_3)(x-\alpha_4)}} \\ &\equiv \frac{1}{\sqrt{C}}F(\varphi, k), \end{aligned} \tag{5.9}$$

where α_1, α_2 are the roots of the equation $x_2 = 0$, while α_3, α_4, for $x_3 = 0$:

$$\begin{aligned} \alpha_{1,2} &= v_0 \pm \left[v_0^2 - u(E - I^2u)\right]^{1/2}, \\ \alpha_{3,4} &= v_0 \pm \left[v_0^2 - E + I^2)\right]^{1/2}. \end{aligned} \tag{5.10}$$

The limits for the integral (5.9) are chosen such that the integrand is a real number for any $x \in (x_{10}, x_1]$. Obviously, the integral (5.9) depends on the relative position of the poles $\alpha_i, i = 1, 2, 3, 4)$. The argument φ involved in the elliptic function is defined as:

$$\varphi = \begin{cases} \arcsin k_1, & if \text{ all } \alpha_{\rm i} \text{ are real}, \\ \arctan k_1, & \text{if two } \alpha_{\rm i} \text{ are complec numbers} \end{cases} \tag{5.11}$$

The explicit expressions of C, k_1^2, k^2 are given in Ref.[55]. Equation (5.9) can be reversed, and the result is a function $x_1(t)$, which is periodic, with the period

$$T = \frac{\pi}{\sqrt{C}}{}_2F_1\left(\frac{1}{2}, \frac{1}{2}, 1; k^2\right). \tag{5.12}$$

In a similar way one may find the functions $x_2(t)$, and $x_3(t)$. The set of points $(x_1(t), x_2(t), x_3(t))|_t$ defines the classical trajectory which can further be quantized. Indeed, let P_0 be an extremal point on the sphere of the radius I, to which the energy E_0 corresponds. Let us now consider the trajectory to be quantized, characterized by the energy E and surrounding P. Consider the calotte bordered by the chosen trajectory, whose area defines the classical action. The quantization consists in restricting the action to be an integer multiple of 2π.

$$\mathcal{L}(E) = \int \Omega = \int_{E_0}^{E}\int_0^T dE'dt' = \int_{E_0}^{E} T(E')E' = 2\pi n. \tag{5.13}$$

From here, one easily finds:

$$\frac{\partial \mathcal{L}}{\partial E} = T(E) = \frac{\partial \mathcal{L}(E)}{\partial n}\frac{\partial E}{\partial n}, \;\; \frac{\partial E}{\partial n} = \frac{2\pi}{T(E)}. \tag{5.14}$$

It results that a linear dependence of E on "n" is obtained when $T(E)$ is approximated by its zero order expansion around E_0. In this case E is given by the harmonic approximation. For an even-even system the period expansion in terms of energy has been performed in Ref.[55].

Here we adopt a different procedure to obtain the harmonic motion of the even-odd system. Several situation are considered:

A1) Indeed, changing the Cartesian to the polar coordinates:

$$x_2 = I\cos\theta_2, \; x_3 = I\sin\theta_2\cos\varphi_2, \; x_1 = I\sin\theta_2\sin\varphi_2, \tag{5.15}$$

which is convenient in the case the maximal MoI corresponds to the 2-axis, the energy function H' can be expressed only in terms of the canonical conjugate coordinates (x_2, φ):

$$\begin{aligned} H' &= x_2^2\left(1 - u\cos^2\varphi_2 - \frac{v_0}{I}\sin\varphi_2\right) \\ &+ uI^2\cos^2\varphi_2 + 2v_0I\sin\varphi_2. \end{aligned} \tag{5.16}$$

The function H' has a minimum in $(x_2, \varphi_2) = (0, -\frac{\pi}{2})$. In the minimum point, the second derivatives of H' have the values:

$$\begin{aligned} \frac{\partial^2 H'}{\partial x_2^2}|_m &= 2\left(1 + \frac{v_0}{I}\right), \\ \frac{\partial^2 H'}{\partial \varphi_2^2}|_m &= 2\left(u + \frac{v_0}{I}\right)I^2. \end{aligned} \tag{5.17}$$

Also the minimal value of H' is:

$$H'|_m = -2v_0I \; . \tag{5.18}$$

Denoting by $(\bar{x}_2, \bar{\varphi})$ the deviation of the current coordinates form those of the minimum point, the second order expansion of H' looks like:

$$H' = -2v_0I + \left(1 + \frac{v_0}{I}\right)\bar{x}_2^2 + \left(u + \frac{v_0}{I}\right)I^2\bar{\varphi}_2^2. \tag{5.19}$$

This describes a harmonic oscillator of a frequency:

$$\omega = 2\sqrt{(1+v)(u+v)I^2}, \tag{5.20}$$

with $v = \frac{v_0}{I}$. By quantization, the spectrum corresponding to H' coincides with that from (4.2), provided the approximation $I + \frac{1}{2} \approx I$ is adopted.

In the minimum point, the angular momentum components are:

$$(x_1, x_2, x_3) = (-I, 0, 0)_m, \tag{5.21}$$

while the energy is: $E_m = -2vI^2$.

A2) One may check that $(0, \frac{\pi}{2})$ is also a minimum of H', in which the angular momentum is $(I, 0, 0)$, while the energy has the expression $E_m = 2vI^2$. The second order expansion of H' is :

$$H' = 2v_0 I + (1-v)\bar{x}_2^2 + I^2(u-v)\bar{\varphi}_2^2. \quad (5.22)$$

This describes an harmonic oscillation of frequency:

$$\omega = 2\sqrt{(1-v)(u-v)I^2}. \quad (5.23)$$

This frequency coincide with the quantal frequency ω' given by Eq.(4.5), if we adopt the approximation $I + \frac{1}{2} \approx I$, which is valid for a large I.

A3) Another pair of conjugate, and stationary variables, which might be minimum for the energy function is:

$$(x_2, \varphi_2)_s = (0, \arcsin\left(\frac{v_0}{Iu}\right)). \quad (5.24)$$

To this, it corresponds the harmonic Hamiltonian;

$$H'_h = uI^2 + \frac{v_0^2}{u} + (1-u)\bar{x}_2^2 - u\left(I^2 - \frac{v_0^2}{u^2}\right)\bar{\varphi}_2^2. \quad (5.25)$$

Obviously, the mentioned stationary point is a saddle point, to which the following angular momentum correspond: $(x_1, x_2, x_3) = (\frac{v_0}{u}, 0, \sqrt{(I^2 - \frac{v_0^2}{u^2})_s}$, with the $E_s = (u + \frac{v^2}{u})I^2$.

B1) Choosing now the 3-axis as quantization axis, and the corresponding polar coordinates:

$$x_1 = I\sin\theta_3\cos\varphi_3,\ x_2 = I\sin\theta_3\sin\varphi_3,\ x_3 = I\cos\theta_3, \quad (5.26)$$

the Hamiltonian H' can be expressed in terms of the canonical conjugate variables (x_3, φ_3):

$$H' = x_3^2\left(u - \sin^2\varphi_3 - \frac{v_0}{I}\cos\varphi_3\right) + I^2\sin^2\varphi_3 + 2v_0 I\cos\varphi_3. \quad (5.27)$$

One stationary point which might be a minimum is $(x_3, \phi_3) = (0, \pi)$. The corresponding angular momentum components are $(x_1, x_2, x_3) = (-I, 0, 0)_m$. Therefore, the angular momentum is oriented along the 1-axis. The minimum energy is $E_m = -2v_0 I$. The harmonic Hamiltonian, i.e. the second order expansion of H' around $(0, \pi)$, is:

$$H'_h = -2v_0 I + \left(u + \frac{v_0}{I}\right)\bar{x}_3^2 + I^2(\left(1 + \frac{v_0}{I}\right)\bar{\varphi}_3^2. \quad (5.28)$$

Although the harmonic Hamiltonian is different from that from the case A), the two scenarios provide the same angular frequencies, but the canonical conjugate variables are interchanged.

B2) Similarly, one shows that $(x_3, \phi_3) = (0, 0)$ is a minimum, which results the quadratic expansion:

$$H'_h = 2v_0 I + \left(u - \frac{v_0}{I}\right)\bar{x}_3^2 + I^2(\left(1 - \frac{v_0}{I}\right)\bar{\varphi}_3^2, \quad (5.29)$$

with the stationary angular momentum $((x_1, x_2, x_3) = (I, 0, 0)_m$, and the corresponding energy $E_m = 2v_0 I$. The harmonic frequency determined by H'_h:

$$\omega = 2\sqrt{(1-v)(u-v)I^2}. \quad (5.30)$$

B3) In this case, the stationary point is $(x_3, \varphi_3) = (0, \arccos\frac{v_0}{I})$, which leads to $(x_1, x_2, x_3) = (v_0, \sqrt{I^2 - v_0^2}, 0)_M$. The corresponding quadratic expansion of H' is:

$$H'_h = I^2 + v_0^2 + (u-1)\bar{x}_3^2 + (v_0^2 - I^2)\bar{\varphi}_3^2, \quad (5.31)$$

which indicates that the stationary point is a maximum point with the critical energy equal to $E_M = I^2(1 + v^2)$.

C1) If the maximal MoI corresponds to the 1-axis, then we choose this as quantization axis, and the polar coordinates:

$$x_1 = I\cos\theta_1,\ x_2 = I\sin\theta_1\cos\varphi_1,\ x_3 = I\sin\theta_1\sin\varphi_1. \quad (5.32)$$

The Hamiltonian becomes:

$$H' = \left(\cos^2\varphi + u\sin^2\varphi\right)\left(I^2 - x_1^2\right) + 2v_0 x_1. \quad (5.33)$$

This has a stationary point in $(x_1, \varphi_1) = \left(\frac{v_0}{u}, \frac{\pi}{2}\right)$. This is a saddle point for H', as suggested by the second order expansion:

$$H'_h = uI + \frac{v_0}{u} - u\bar{x}_1^2 + (1-u)\left(I^2 - \frac{v_0^2}{u^2}\right)\bar{\varphi}_1. \quad (5.34)$$

The corresponding angular momentum and energy are: $(x_1, x_2, x_3) = (\frac{v_0}{u}, 0, \sqrt{(I^2 - \frac{v_0^2}{u^2})_s}$, and $E_s = (u + \frac{v^2}{u})I^2$.

C2) The stationary point $(v_0, 0)$ is a maximum, with the angular momentum $(x_1, x_2, x_3) = (v_0, \sqrt{I^2 - v_0^2}, 0)_M$, and energy $E_M = I^2 + v_0^2$. The quadratic expansion around this point is:

$$H'_h = I^2 + v_0^2 - \bar{x}_1^2 + (u-1)(I^2 - v_0^2)\bar{\varphi}_1^2. \quad (5.35)$$

Concluding this analysis, there are four minima, the cases A1), A2), B1), and B2), one maximum, the cases B3),C2), and one saddle point, the situations A3) and C1). The frequencies corresponding to the four minima are grouped in two pairs of degenerate frequencies, and moreover the frequency showing up in the cases A1), and B1) is equal to the one provided by the quantal description for the deepest minimum of the potential energy. The other two degenerate minima, A2) and B2) produce a frequency equal to the one showing up in the quantal description, and the local minimum. In the minimum points, the total angular momentum is oriented along a principal axis,namely the 1-axis, while for the maximum and the saddle point is located in a principal plane. It is worth mentioning that in the maximum point, the angular momentum is oriented along the 2-axis to which the maximal MoI corresponds. Therefore, the transverse wobbling is unstable.

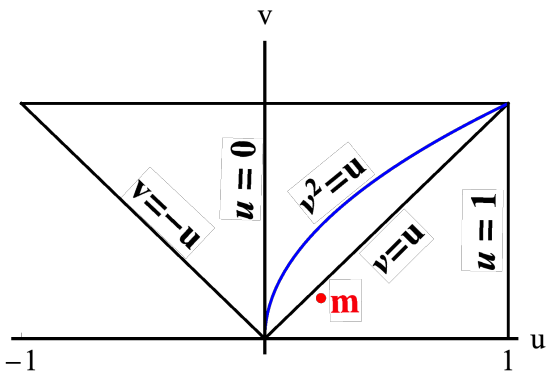

FIG. 7: (Color online) The phase diagram for I=15/2 of ^{135}Pr. Using the MoI's, and θ determined by the adopted fitting procedure, and $\theta = 150^0$, we mentioned the minimum point by a red and full circle having a lowercase m.

A. The phase diagram

The character of the stationary point to be minimum, maximum or saddle point is decided by the signs of the diagonal matrix elements of the Hessian: a) if all diagonal elements are positive, the stationary point is minimum; b) if all diagonal m.e. are negative, then we deal with a maximum, while; c) is a saddle point if one m.e. is positive and the other is negative. Equating the Hessian to zero, one obtains the parameters u, and v for which the critical points are degenerate. The resulting equations may be unified in a single formulae:

$$(1-u)(1-v^2)(v^2-u^2)(v^2-u) = 0. \tag{5.36}$$

The last factor in the above equation is obtained by equating the critical energies E_M, and E_s. Each factor generates a curve, called separatrice, in the parameter space spanned by (u,v). As shown in Fig. 7, the separatrices are bordering manifolds defining unique nuclear phases characterized by a specific portrait of the stationary points. Indeed, among the factors involved in Eq.(5.36), we recognize those defining the two wobbling frequencies. On the other hand a vanishing energy defines a Goldstone mode [41] which, as a matter of fact, render evidently a phase transition.

VI. ELECTROMAGNETIC TRANSITIONS

We are interested in describing the experimental data for the electric quadrupole intra- and inter-band transitions as well as the magnetic dipole transitions. We begin with the electric transitions. Aiming at this goal, we need the wave functions describing the involved states, and the transition quadrupole operator. The wave function for an I-state is the solution of the Scrödinger equation for the given total angular momentum, I. Note that the wave function is degenerate with respect to "M", the projection of I on the x-axis, in the laboratory frame. Since the ground state is the vacuum state for the wobbling phonon operator, and moreover, in the minimum point of the constant energy surface, the a.m. projection on the one-axis of the intrinsic frame is equal to -I, it results that the K quantum number is equal to -I. Therefore the solution of the Schrödinger equation must be labelled by the mentioned quantum numbers, i.e.

$$\begin{aligned} \Psi_{IM} &= \Phi_{I,-I}|IM,-I\rangle, \text{ with} \\ |IMK\rangle &= \sqrt{\frac{2I+1}{8\pi^2}}D^I_{M,K}. \end{aligned} \tag{6.1}$$

Here we consider the first two wobbling bands as signature partner bands, the arguments being in detail given in Ref.[27]. More specifically, the spin sequence of the first band is $j+R$, for R=0,2,4,... , while for the second band the spin succession is $j+R$, with R=1,3,5,.... Note that the quadrupole inter-band transition is forbidden since, for the states mentioned above, have $\Delta K = 1$. In this case, considering the component $K = -I+1$ in one of the involved states is necessary. The quadrupole transition operator is taken as:

$$\mathcal{M}(E2;\mu) = \sqrt{\frac{5}{16\pi}}e\left(Q_0 D^2_{\mu 0} + Q_2\left(D^2_{\mu 2} + D^2_{\mu -2}\right)\right), \tag{6.2}$$

where Q_0, and Q_2, denote the $K=0$, and $K=\pm 2$ components of the quadrupole transition operator, respectively. Note that since the intrinsic component of the wave function depends on one of the conjugate variables q, and d/dq, that is q, we must express the quadrupole operators in terms of the q variable. This will be achieved by writing Q-s in the space of angular momentum and then use the Bargmann representation of the a.m. components. Thus we have:

$$\begin{aligned} Q_0 &= -\frac{1}{4}\sqrt{\frac{2}{3}}\left(\hat{I}_+\hat{I}_- + \hat{I}_-\hat{I}_+\right) + \sqrt{\frac{2}{3}}\hat{I}_1^2, \\ Q_2 &= \frac{1}{2}\left(\hat{I}_+^2 + \hat{I}_-^2\right). \end{aligned} \tag{6.3}$$

In the next step, the a.m. components $\hat{I}_\pm$, and $\hat{I}_0$ are written in the Bargmann representation, and then the derivative coefficients expanded in the second order around the minimum point of the energy. The result is:

$$\begin{aligned} Q_0 &= \frac{1}{\sqrt{6}}\left[3\bar{q}^2\frac{d^2}{d\bar{q}^2} - 3(2I-1)\bar{q}\frac{d}{d\bar{q}}\right. \\ &+ \left. I(2I-1) - I(I-1)(1+k^2)\bar{q}^2\right], \\ Q_2 &= \frac{1}{k'^2}\left\{\left[-2+(1+k^2)\bar{q}^2\right]\frac{d^2}{d\bar{q}^2} - (2I-1)(1+k^2)\bar{q}\frac{d}{d\bar{q}}\right. \\ &- \left. I(1+k^2) + I\left[(I+1)(1+k^2) + k^2(k^2+3)\right]\bar{q}^2\right\}. \end{aligned} \tag{6.4}$$

Note that the magnitude $k(=\sqrt{u})$, defined by Eq. (2.10), depends on the angular momentum I due to u. Therefore, hereafter, we attach to it a lower index specifying this dependence. The same procedure is used for he

$K+1$, and $K+2$ wave-functions:

$$\Phi_{I,-I+1} \equiv \frac{\mathcal{N}_I^{(1)}}{\sqrt{2I}}\hat{I}_-\Phi_{I,-I} = ik_I'\frac{\mathcal{N}_I^{(1)}}{\sqrt{2I}} \tag{6.5}$$
$$\times \left(-I\bar{q}+\frac{\bar{\omega}_I}{4}\bar{q}^3\right)\Phi_{I,-I}, \text{ with } \mathcal{N}_{\rm I}^{(1)} = \frac{1}{\rm k_I'}\sqrt{\frac{\bar{\omega}_{\rm I}}{\rm I}},$$
$$\Phi_{I,-I+2} \equiv \frac{\mathcal{N}_I^{(2)}}{\sqrt{4I(2I-1)}}\hat{I}_-^2\Phi_{I,-I} = \frac{-\mathcal{N}_I^{(2)}k_I'}{2\sqrt{I(2I-1)}}$$
$$\times \left(-I\bar{q}+\frac{1}{2}\bar{q}^2\frac{d}{d\bar{q}}\right)^2\Phi_{I,-I},\ \mathcal{N}_I^{(2)} = \frac{2\bar{\omega}_I}{k_I'^2\sqrt{I(2I-1)}}.$$

The state describing the oscillator vacuum is

$$\Phi_{I,-I} = C_I e^{-\frac{1}{2b_I^2}\bar{q}^2}, \tag{6.6}$$

where the norm, and the oscillator length are:

$$C_I = \sqrt{\frac{2}{\pi}}\frac{1}{b_I},\ \ b_I^2 = \frac{\hbar}{M\bar{\omega}_I}. \tag{6.7}$$

In our case, the units system is that where $\hbar = 1$, while the mass parameter is $M = \frac{1}{2}$. Therefore

$$b_I = \sqrt{\frac{2}{\bar{\omega}_I}}, \tag{6.8}$$

where $\bar{\omega}_I$ is defined by Eq.(4.2) or by (4.4), and $\bar{\omega}_I = \omega_I/A$. With the above ingredients, the m.e. of the transition operator corresponding to the intrisic states $|\Phi_{I,-I}\rangle$ can be evaluated by integration.

However, here we propose an alternative version for the necessary matrix elements, which actually will be used in our concrete calculations. We use the expression (6.3), and evaluate directly the acting on the system wave function with the spherical components of $\mathbf{I}$. The nice feature of this procedure is that any reduced m.e. is expressed by a factor multiplying the overlap of the initial, and final intrinsic states. For example, for inter-band transitions, this overlap is:

$$\langle\Phi_{I,-I}|\Phi_{I-1,-I+1}\rangle = \frac{2\sqrt{\bar{\omega}_I\bar{\omega}_{I-1}}}{\bar{\omega}_I+\bar{\omega}_{I-1}}. \tag{6.9}$$

Thus, the matrix elements involved in the equation defining the reduced transition probabilities are analytically expressed as given in Appendix A

The matrix elements for the intra-band transitions are:

$$\langle\Psi_I||\mathcal{M}(E2)||\Psi_{I-2}\rangle = \sqrt{\frac{5}{16\pi}}e\left[\bar{Q}_2C^{I\ 2\ I-2}_{I-2\,I-2}\right.$$
$$\times \left(\langle\Phi_{I,-I}|Q_2|\Phi_{I-2,-I+4)}\rangle + \langle\Phi_{I,-I+2}|Q_2|\Phi_{I-2,-I+2}\rangle\right)$$
$$+ \left.\bar{Q}_0C^{I\ 2\ I-2}_{I-2\,0\,I-2}\langle\Phi_{I,-I+2}|Q_0|\Phi_{I-2,-I+2)}\rangle\right], \tag{6.10}$$

while those determining the inter-band transitions have

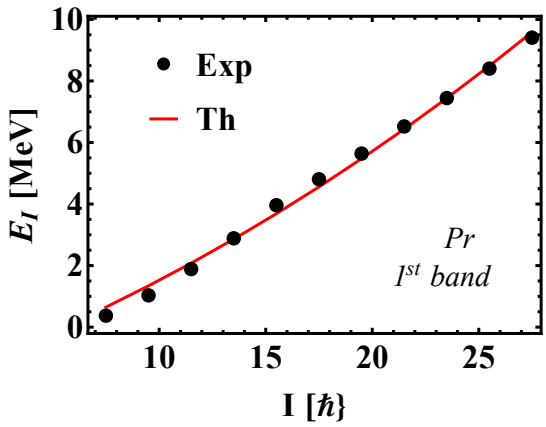

FIG. 8: (Color online) The excitation energies yielded by our calculations for the yrast band of ^{135}Pr, using the MoI's, and θ determined by a fitting procedure.

the expressions [61]:

$$\langle\Psi_I||\mathcal{M}(E2)||\Psi_{I-1}\rangle = \sqrt{\frac{5}{16\pi}}e\left[\bar{Q}_2C^{I\ 2\ I-1}_{I-1\ -2\ I-3}\right.$$
$$\times \left(\langle\Phi_{I,-I}|Q_2|\Phi_{I-1,-I+3}\rangle + \langle\Phi_{I,-I+2}|Q_2|\Phi_{I-1,-I+1}\rangle\right),$$
$$+ \left.\bar{Q}_0C^{I2I-1}_{I-10I-1}(\langle\Phi_{I,-I+1}|Q_0|\Phi_{I-1,-I+1}\rangle\right],$$
$$\langle\Psi_I||\mathcal{M}(E2)||\Psi_{I+1}\rangle = \sqrt{\frac{5}{16\pi}}e\left[\bar{Q}_2C^{I\ 2\ I+1}_{I\ -2\ I-2}\right.$$
$$\times \left(\langle\Phi_{I,-I}|Q_2|\Phi_{I+1,-I+1}\rangle + \langle\Phi_{I,-I+2}|Q_2|\Phi_{I+1,-I-1}\rangle\right)$$
$$+ \left.\bar{Q}_0C^{I\ 2\ I+1}_{I\ 0\ I}(\langle\Phi_{I,-I}|Q_0|\Phi_{I+1,-I-1}\rangle\right]. \tag{6.11}$$

Furthermore, the reduced transition probabilities are readily obtained:

$$B(E2;I\to I') = \left[\langle\Psi_I||\mathcal{M}(E2)||\Psi_{I'}\rangle\right]^2. \tag{6.12}$$

The factors $\bar{Q}_0$, and $\bar{Q}_2$ have the units of e.fm$^2/\hbar^2$, and are taken as free parameters.

The magnetic dipole transition operator is:

$$\mathcal{M}(M1;\mu) = \sqrt{\frac{3}{4\pi}}\mu_N\sum_\nu\left(g_R\hat{R}_\nu + g_j\hat{j}_\nu\right)D^1_{\mu\nu},$$
$$\equiv M^{coll}_{1\mu} + M^{sp}_{1\mu}, \tag{6.13}$$

where R_ν, and j_ν are the spherical components of the core and the odd nucleon angular momenta, respectively. g_R and g_j stand for the gyromagnetic factors of the core, and the coupled odd nucleon, respectively. Also, the standard notation for the Wigner function, D^J_{MK}, and for the nuclear magneton, μ_N, are used. To calculate the collective part of the transition matrix element, we need to express the wave function describing the odd system as a Kronecker product of the core, and the odd particle wave functions:

$$|IMK\rangle = \frac{1}{2j+1}\sum_{M_R,\Omega,R}C^{R\ j\ I}_{M_R\ \Omega\ M}|RM_RK\rangle\psi_{j\Omega}. \tag{6.14}$$

By a direct manipulation, one finds:

$$\langle I||M_1^{coll}||I-1\rangle = -\sqrt{\frac{3}{4\pi}}g_R\mu_N\frac{1}{2j+1}C^{I+j-11I+j-1}_{I+j-21I+j-1}$$
$$\times\ [(2I-1)(2J+2j-1)(I+j-1)(I+j)]^{1/2}\ \frac{\sqrt{\bar{\omega}_I\bar{\omega}_{I-1}}}{\bar{\omega}_I+\bar{\omega}_{I-1}}$$
$$\times\ W(I-1,j,1,I+j;I+j-1,I), \qquad (6.15)$$

where the notation $W(a,b,c,d;e,f)$ stands for the Racah coefficient.

To calculate the reduced m.e. of the single particle M1 operator we need the wave function describing the odd proton whose a.m. is placed in the plane XOY making the angle θ with the axis OX. This function is obtained by rotating around the axis 3, the function $\psi_{j,j}$ associated to the odd proton having the a.m. along the 1-axis.

$$\psi'_j = R_3(\theta)\psi_{jj}. \qquad (6.16)$$

The reduced m.e. of the single particle transition operator is:

$$\langle I||M_1^{sp}||I-1\rangle = \sqrt{\frac{3}{4\pi}}g_j\mu_N$$
$$\times\ C^{I\ 1\ I-1}_{I\ -1\ -I}\langle\psi_{jj}|R_3^\dagger(\theta)j_{-1}R_3(\theta)|\psi_{jj}\rangle$$
$$=\ \frac{1}{\sqrt{2}}\langle\psi_{jj}|-\hat{j}_1\sin\theta+\hat{j}_+\frac{\cos\theta-1}{2}+\hat{j}_-\frac{\cos\theta+1}{2}|\psi_{jj}\rangle$$
$$=\ -j\sin\theta\sqrt{\frac{3}{8\pi}}\mu_N g_j C^{I\ 1\ I-1}_{I\ -1\ -I}. \qquad (6.17)$$

The gyromagnetic factors have the expressions:

$$g_R=\frac{Z}{A},\ g_j=g_l+\frac{\frac{3}{4}+j(j+1)-l(l+1)}{j(j+1)}\frac{g_s-g_l}{2}, \qquad (6.18)$$

where g_l, and g_s stand for the orbital and spin free gyromagnetic factors, respectively. Finally, the magnetic dipole reduced transition probability is given by:

$$B(M1;I\to I')=\left[\langle\Psi_I||\mathcal{M}(M1)||\Psi_{I'}\rangle\right]^2. \qquad (6.19)$$

VII. RESULTS

The formalism described in the previous sections was applied to ^{135}Pr. The excitation energies in three bands, conventionally called band 1 (B1), band 2 (B2), and band 3 (B3), and the electromagnetic properties of the states have been described by a simple Hamiltonian (2.1), associated to the even-even core and the odd proton, which stays in the orbital $h_{11/2}$.The core properties are simulated by a triaxial core with the moments of inertia $\mathcal{J}_k$ (k=1,2,3), considered to be free parameters, while the odd proton is rigidly coupled to the core and having the angular momentum $j=11/2$, placed in the inertial plane (1,2), and having the polar angle θ. Thus, the approach involves four free parameters $\mathcal{J}_k$ (k=1,2,3), and θ, which were fixed by a least mean square procedure, fitting the excitation energies for the three bands.

A. Energies

The excitation energies for the first three bands are obtained from Eq.(4.3):

$$\begin{aligned}
E_I^{exc;1} &= A_1I^2+(2I+1)A_1j_1-IA_2j_2+\omega_I/2-E_{11/2},\\
I &= R+j,\ \ R=0,2,4,...,\\
E_I^{exc;2} &= A_1I^2+(2I+1)A_1j_1-IA_2j_2+\omega_I/2-E_{11/2},\\
I &= R+j,\ \ R=1,3,5,...,\\
E_{I+1}^{exc;3} &= A_1I^2+(2I+1)A_1j_1-IA_2j_2+3\omega_I/2-E_{11/2},\\
I &= R+j,\ \ R=1,3,5,....
\end{aligned} \qquad (7.1)$$

As we already mentioned, the involved parameters were fixed by fitting the experimental excitation energies with those described by the above equations. The parameters yielded by the fitting procedure are listed in Table I. With the parameters thus determined, and Eq.(7.1), the excitation energies are readily obtained. They are visualized in Figs.7, 8, 9 and compared with the corresponding experimental data taken from Refs.[33, 34]. From there, one sees the quality of the agreement with the data, that might be appraised by the r.m.s. of the deviation which is also given in Table I. We may conclude that the agreement between theoretical, and experimental results is good.

$\mathcal{I}_1$ $[\hbar^2/MeV]$	$\mathcal{I}_2$ $[\hbar^2/MeV]$	$\mathcal{I}_3$ $[\hbar^2/MeV]$	θ [degrees]	nr. of states	r.m.s. [MeV]
89	12	48	-71	20	0.174

TABLE I: The MoI's, and the parameter θ as provided by the adopted fitting procedure.

From Table I we see that the MoI's ordering predicted by our calculations is: $\mathcal{J}_1>\mathcal{J}_3>\mathcal{J}_2$. However, due to the adopted fitting procedure this, however, is a global result. In order to check whether this ordering holds also by using another fitting procedure, we fixed the MoI's by equating the calculated excitation energies for the lowest two states of band 1 and the second state of band 2, otherwise fixing θ to obtain a global best fit. In this way we found a set of MoI,s which reclaims a transverse wobbling regime for the odd system under consideration. Indeed, for $\theta=140^0$, the result is $\mathcal{J}_1=13.5285[\hbar^2/MeV]$, $\mathcal{J}_2=$

	$\frac{B(E2;I^-\to(I-1)^-)}{B(E2;I^-\to(I-2)^-)}$		$\frac{B(M1;I^-\to(I-1)^-)}{B(E2;I^-\to(I-2)^-)}[\frac{\mu_N^2}{e^2b^2}]$		$\delta_{I^-\to(I-1)^-}$ [MeV.fm]	
I^π	Exp.	Th.	Exp.	Th.	Exp.	Th.
$\frac{21}{2}^-$	0.843±0.032	0.510	0.164± 0.014	0.164	-1.54± 0.09	-0.542
$\frac{25}{2}^-$	0.500±0.025	0.500	0.035± 0.009	0.066	-2.384±0.37	-0.703
$\frac{29}{2}^-$	≥0.261±0.014	0.487	≤ 0.016±0.004	0.033	-	-0.873
$\frac{33}{2}^-$	-	0.473	-	0.019	-	-1.052

TABLE II: The calculated branching ratios $B(E2)_{out}/B(E2)_{in}$, and $B(M1)_{out}/B(E2)_{in}$ as well as the mixing ratios δ are compared with the corresponding experimental data taken from Ref. [33].

labelTable II

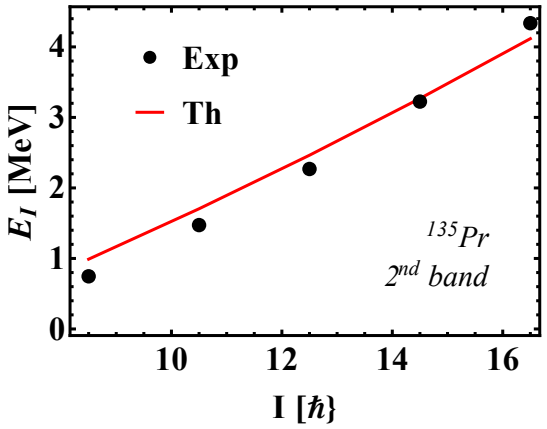

FIG. 9: (Color online) The excitation energies for the second band of ^{135}Pr, with the parameters determined as explained in the text.

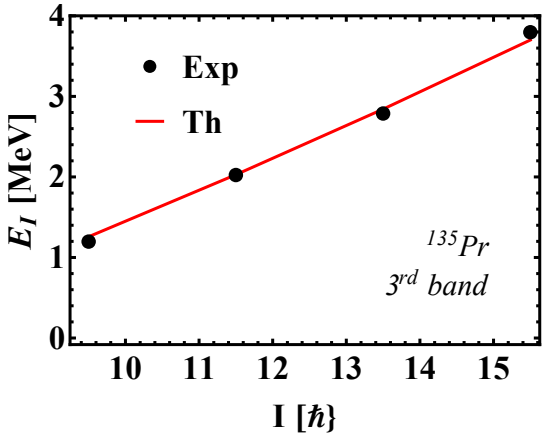

FIG. 10: (Color online) The excitation energies for the one phonon band of ^{135}Pr, with the parameters determined as explained in the text.

$101.759[\hbar^2/MeV]$, $\mathcal{J}_3 = 52.9364[\hbar^2/MeV]$. However, the overall agreement is of a poor quality. We also plotted the potential determined by the fitted parameters and I=19/2. The result is of the type given in Fig.5, i.e., the deepest minimum is placed at $q = 0$. In this point $I_1 = I$, which means that the angular momentum is oriented along the axis one. Therefore, $\mathcal{J}_2$= maximal, does not necessarily mean that the rotation axis is the 2-axis. The fact that the maximal MoI established by a global fit is $\mathcal{J}_1$, indicates that for a larger angular momentum a change of MoI hierarchy takes place, and a new nuclear phase begins.

B. Comment on the chiral features of the wobbling motion

We recall that a chiral transformation brings a right-handed reference frame to a left-handed one. In the angular momentum space, the change of sign of the a.m. defines a chiral transformation. A system is invariant to a chiral transformation if its rotational energy is preserved when the sense of rotation around an axis is changed. Note that our starting Hamiltonian is a sum of two terms, one being symmetric to chiral transformations, and one antisymmetric to chiral transformations.

$$\hat{H}_{rot} = \hat{H}_s + \hat{H}_a. \tag{7.2}$$

If $|\psi\rangle$ is an eigenstate for $\hat{H}_s$, and C is a chiral transformation, then $C|\psi\rangle$ is also eigenstate for $\hat{H}_s$, and corresponds to the same energy. In this case, the function $|\psi\rangle$ has the chirality equal to one, since $C\psi\rangle = \psi\rangle$. For $\hat{H}_a$, the above mentioned property changes to : If $|\psi\rangle$ is an eigenstate of $\hat{H}_a$ corresponding to the eigenvalue E, then $C\psi\rangle$ is also eigenstate, but corresponding to the energy $-E$. Therefore, the eigenvalues of $\hat{H}_a$ split in two sets, one being the mirror image of the other one. This property is of a chiral nature. The eigenstates of $\hat{H}_a$ have the chirality -1 since $C|\psi\rangle = -|\psi\rangle$. The eigenstates of $\hat{H}_{rot}$ are mixtures of the two chiralities. When there are two sets of energies that are one the mirror image of the other, one says that a definite chirality is projected out [22]. In our calculation, the change of $\mathbf{I} \to -\mathbf{I}$ is achieved by changing θ to $\theta+\pi$. The a.m. dependence of the wobbling frequencies corresponding to $\theta = -71^0$, and $\theta = 109^0$ respectively, is shown in Fig. 11. The look of the potentials V, and CVC^{-1}, are shown in Figs.4 and 5 for $\theta = \pi/6$, and $\theta = 7\pi/6$ respectively, and $\mathcal{J}_1 : \mathcal{J}_2 : \mathcal{J}_3 = 100 : 40 : 20\hbar^2 MeV^{-1}$. From these two potentials we may extract the symmetric, and

antisymmetric parts of V.

$$V_s = \frac{1}{2}V(\pi/6) + V(7\pi/6); \;\; V_a = \frac{1}{2}V(\pi/6) - V(7\pi/6). \tag{7.3}$$

The two potential of definite chirality, are visualized in Fig. 12 and fig.13, respectively. A similar analysis can be performed also for the excitation energies. Indeed, Eq.(4.4) expresses explicitly the dependence of the wobbling frequency on the angle θ, which fixes the orientation of **j**. Therefore, it is easy to calculate $\omega_I(\theta+\pi)$, with $\theta = -71^0$. The frequencies $\omega_I(\theta)$, and $\omega_I(\theta+\pi)$, with one being the chiral image of the other one, are plotted in Fig.11 for the yrast band. The two curves are parallel to each other, which suggests that the corresponding states have similar properties. However, they do not correspond to states of definite chirality. However, one can extract the symmetric, and antisymmetric terms of the excitation energy. Here we give the result for the yrast states:

$$\begin{aligned} &E^{exc;1}_{I,s} = A_1 I^2 + \left(\omega_I(\theta) + \omega_I(\theta+\pi)\right)/2 - E_{11/2}, \\ &I = R + j, \;\; R = 0, 2, 4, .. \\ &E^{exc;1}_{I,a} = (2I+1)A_1 j_1 - I A_2 j_2 + \left(\omega_I(\theta) - \omega_I(\theta+\pi)\right)/2, \\ &I = R + j, \;\; R = 0, 2, 4, .., \theta = -71^0. \end{aligned} \tag{7.4}$$

Since for asymmetric states, the energies $-E^{exc;1}_{I,a}$ are also eigenvalues of the antisymmetric Hamiltonian, we interpret the two sets of energies $E^{exc;1}_{I,s}$, and $-E^{exc;1}_{I,a}$ as defining two bands of chirality +1, and -1, respectively. The relative energies to the head-energy of each band respectively, are plotted in Fig.14. Although the two sets of energies have different dependence on the angular momentum, one is linear (asymmetric) and the other one quadratic in a.m., the energy spacing in the two bands are close to each other, which in fact is a chiral feature of the two bands. Although we don't have enough data to conclude that the two bands are indeed of real chiral type, however, due to the above mentined features, they might be considered as germinos of chiral bands. Indeed, there are properties unanimously accepted, which prevent us to make a decisive statement on this matter. For a chiral band the system rotates around an axis, which doesn't belong to any of principal planes, while here the rotation axis is a principal axis. However, since in our case the Hamiltonian involves linear terms in the total angular momentum, the wobbling motion, and chiral properties seem not to be disconnected.

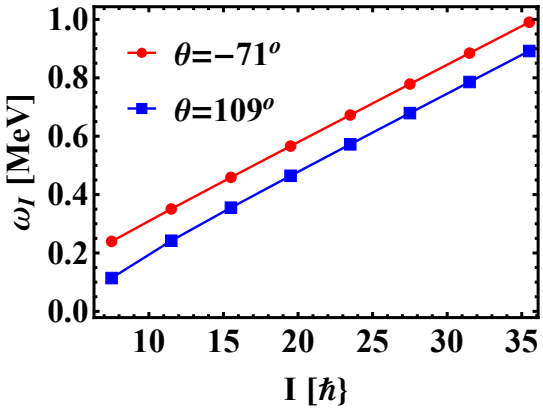

FIG. 11: (Color online) The wobbling frequencies corresponding to the angles $\theta = 109^0$, and $\theta = -71^0$, respectively.

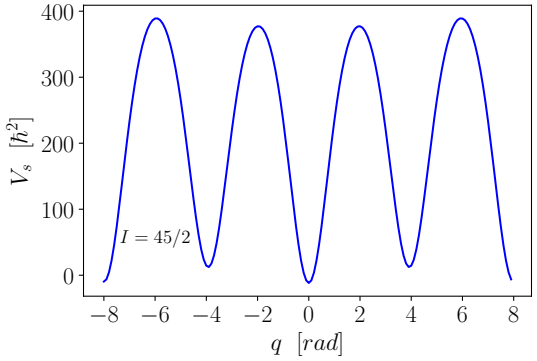

FIG. 12: (Color online) The symmetric potential, with respect to the chiral transformations, as function of q.

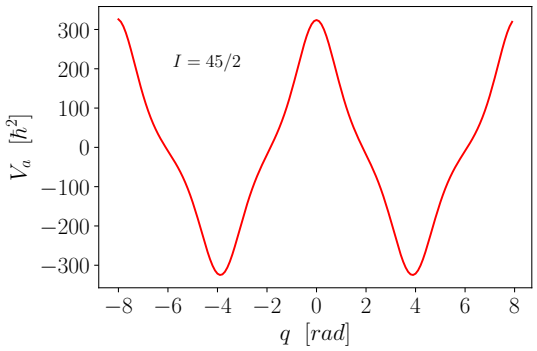

FIG. 13: (Color online) The antisymmetric potential, with respect to the chiral transformations, as function of q.

C. Electromagnetic traditions

The electric quadrupole reduced transition probabilities were calculated by means of Eq. (6.11), where the reduced matrix elements are those given by (6.10) for the intra-band, and (6.11), for the inter-band transitions. These expressions involve two strength parameters of the quadrupole transition operator, denoted by $\bar{Q}_0$, and $\bar{Q}_2$, respectively. These were determined by fitting two particular branching ratios which results in obtaining the values: $\bar{Q}_0 = 13.3888 \; e.fm^2/\hbar^2$, and $\bar{Q}_2 = 149.9093 \; e.fm^2/\hbar^2$. The results are given in Table II, where the available corresponding experimental data [33] are also listed. One notices a reasonable good agreement between the results of our calculations, and the experimental data. The increasing function of the a.m. for

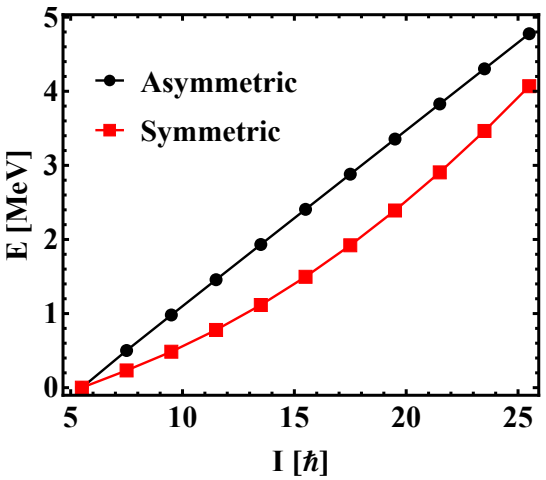

FIG. 14: (Color online)Energies of symmetric and antisymmetric states against chiral transformations, normalized to the head-energy for each band.

the ratio $B(E)_{out}/B(E)_{in}$ is well reproduced. Also, the sign of the mixing ratio, and the increasing behavior with I, are also consistent with the data, although the magnitudes of the experimental data exceed the calculated values by a factor of about 3.

VIII. CONCLUSIONS

The formalism developed in the previous sections may be summarized as follows. A new boson expansion is proposed to describe the wobbling motion in even-odd nuclei. The used Hamiltonian has a simple structure obtained from that describing the even-even core, i.e., a triaxial rotor, by replacing the core angular momentum $\mathbf{R}$ with $\mathbf{I}-\mathbf{j}$, where $\mathbf{I}$ and $\mathbf{j}$ denote the total and odd particle angular momenta, respectively. The coupling term, describing the motion of the odd nucleon in a deformed mean field generated by the core [48] is ignored, since we suppose that the odd particle is rigidly coupled to the core, and thereby does not affect the excitation energy spectrum for the odd system. The model Hamiltonian is written in a boson space by using for angular momentum an "elliptic expansion". Subsequently, the Bargmann representation is employed, and the eigenvalue equation of the initial model Hamiltonian is brought to a Schrödinger equation form, where the kinetic, and potential energy terms are fully separated. The potential is angular momentum dependent, and exhibits several minima, and maxima. Expanding, successively, the potential around the deepest, and the local minima, one arrives at two distinct expressions for the wobbling frequency. These results are also obtained within a classical picture, where the phase diagram is constructed for a particular value of I(=15/2). The frequency associated to the deepest minimum is used to describe the energies of the three bands seen in ^{135}Pr. Due to the presence of linear terms in the model Hamiltonian, a possible chiral behavior for the odd system is expected. One succeeds to build up states of a definite chirality. However, it is hard to call the resulting bands as twin bands, although some embryos of them are present. The electromagnetic reduced transition probabilities are calculated by using for the quadrupole transition operator a quadratic form in the angular momentum. Results for the branching ratios $B(E2)_{out}/B(E2)_{in}$, and $B(M1)_{out}/B(E2)_{in}$, as well as for the mixing ratios δ, are compared with the available data. One concludes that the agreement with experimental data for both energies, and e.m. transitions is reasonable good. It was pointed out that, although we started with the hypothesis that the maximal MoI is that of 2-axis, the fitting procedure yielded as maximal MoI that of 1-axis. There is a two fold reason causing that:a) the renormalization of the MoI, due to the linear terms in angular momentum; and b) the Coriolis interaction simulated by the term proportional to I_1. At classical level, one showed that the transverse wobbling motion is unstable.

We may assert that the results of the present paper confirm the importance of the boson expansion concept, which was widely used in different contexts of theoretical nuclear physics [57–60].

Concluding, the present formalism is an interesting tool to investigate the theoretical aspects of the wobbling motion in even-odd nuclei, and also to describe the existent data in a realistic fashion.

Acknowledgment. This work was supported by the Romanian Ministry of Research and Innovation through the project PN19060101/2019

IX. APPENDIX A

Here we list the analytical expressions for the matrices involved in the quadrupole transition probabilities. The result are as follows:

$$\begin{aligned}
\langle I,-I|Q_2|I-1,-I+3\rangle &= \sqrt{(2I-3)(I-1)}\frac{2\sqrt{\bar{\omega}_I*\bar{\omega}_{I-1}}}{\bar{\omega}_I+\bar{\omega}_{I-1}},\\
\langle I,-I+2|Q_2|I-1,-I+1\rangle &= \sqrt{I(2I-1)}\frac{2\sqrt{\bar{\omega}_I*\bar{\omega}_{I-1}}}{\bar{\omega}_I+\bar{\omega}_{I-1}},\\
\langle I,-I|Q_2|I-2,-I+4\rangle &= \sqrt{(I-2)(2I-5)}\frac{2\sqrt{\bar{\omega}_I*\bar{\omega}_{I-2}}}{\bar{\omega}_I*\bar{\omega}_{I-2}},\\
\langle I,-I+2|Q_2|I-2,-I+2\rangle &= \sqrt{I(2I-1)}\frac{2\sqrt{\bar{\omega}_I*\bar{\omega}_{I-2}}}{\bar{\omega}_I*\bar{\omega}_{I-2}},\\
\langle I,-I|Q_2|I+1,-I+1\rangle &= \sqrt{(2I+1)(I+1)}\frac{2\sqrt{\bar{\omega}_I*\bar{\omega}_{I+1}}}{\bar{\omega}_I*\bar{\omega}_{I+1}},
\end{aligned} \tag{A.1}$$

$$\langle I,-I+2|Q_2|I+1,-I-1\rangle=\sqrt{I(2I-1)}\frac{2\sqrt{\bar{\omega}_I*\bar{\omega}_{I+1}}}{\bar{\omega}_I*\bar{\omega}_{I+1}},\ \langle I,-I|Q_0|I-1,-I+1\rangle=\frac{1}{24}\left(4I^2-6I+3\right)\frac{2\sqrt{\bar{\omega}_I*\bar{\omega}_{I-1}}}{\bar{\omega}_I+\bar{\omega}_{I-1}},$$

$$\langle I,-I|Q_0|I-2,-I+2\rangle=\frac{1}{6}\left(2I^2-5I+5\right)\frac{2\sqrt{\bar{\omega}_I*\bar{\omega}_{I-2}}}{\bar{\omega}_I+\bar{\omega}_{I-2}},\langle I,-I|Q_0|I+1,-I-1\rangle=\frac{1}{24}\left(4I^2+2I+1\right)\cdot\frac{2\sqrt{\bar{\omega}_I*\bar{\omega}_{I+1}}}{\bar{\omega}_I+\bar{\omega}_{I+1}}.$$

[1] A. Bohr and B. Mottelson, *Nuclear Structure* (Benjamin, Reading, MA, 1975), Vol. II, Ch. 4.
[2] E. R. Marshalek, Nucl. Phys. **A 331**, 429, (1979).
[3] S. W. Odegard, *et al.*, Phys. Rev. Lett. **86**, 5866, (2001).
[4] D. R. Jensen *et al.*, Nucl. Phys. **A 703**, 3, (2002).
[5] I. Hamamoto *et al.* Acta. Phys. Pol. **B32**, 2545, (2001).
[6] G. Schoenwasser *et al.*, Phys. Lett. **B 552**,9, (2003).
[7] H. Amro *et al.*, Phys. Lett. **B 553**, 197, (2003).
[8] A. Görgen et al., Phys. Rev **C 69**, 031301(R), (2004).
[9] I. Hamamoto, Phys. Rev. **C 65**, 044305, (2002).
[10] M. Matsuzaki, Y. R. Shimizu, K. Matsuyanagi, Phys. Rev. **C 65**, 041303(R), (2002); Yoshifumi R. Shimizu, Masayuki Matsuzaki and Kenichi Matsuyanagi,arXiv:nucl-th/0404063v1, 22 Apr. 2004.
[11] I. Hamamoto and G. B. Hagemann, Phys. Rev. **C 67**, 014319, (2003).
[12] D. R. Jensen *et al.*, Eur. Phys. J. **A 19**, 173, (2004).
[13] G. B. Hagemann, Eur. Phys. J. **A 20**, 183, (2004).
[14] K. Tanabe and K. Sugawara-Tanabe, Phys. Rev. **C73**, 034305, (2006).
[15] Makito Oi, Phys. Lett. **B 634**, 30 (2006).
[16] A. A. Raduta, R. Budaca and C. M. Raduta, Phys. Rev. C, **76**, 064309,(2007).
[17] P. Bringel *et al.* Eur. Phys. J. **A 24**, 167, (2005).
[18] D. J. Hartley *et al.*, Phys. Rev. **C 80**, 041304(R), (2009).
[19] R.F. Casten, E. A. McCutchan, N. V. Zamfir, C. W. Beausuang and Jing-ye Zhang, Phys. Rev. **C 67**, 064306, (2003).
[20] D. Almehed, R. G. Nazmitdinov and F. Dönau, Phys. Scr. **T125**, 139, (2006).
[21] I. N. Mikhailov and D. Janssen, Phys. Lett. **72B**, 303, (1978).
[22] A. A. Raduta, Progress in Particle and Nuclear Physics 90, 241, (2016).
[23] M.Badea and A. A. Raduta, Rev. Roum. Phys. 21 , 743, (1979).
[24] A. A. Raduta, R. Poenaru and L. Gr. Ixaru, Phys. Rev. C **96**, 054320, (2017).
[25] A. A. Raduta, R. Poenaru and Al. H. Raduta, J. Phys. G: Nucl. Part. Phys. **45** 105104 (2018).
[26] A. A. Raduta, R Poenaru and C M Raduta, J. Phys. G: Nucl. Part. Phys. **47**,025101 (2020).
[27] A. A. Raduta, R Poenaru and C M Raduta, Phys. Rev. C **101**, 014302 (2020).
[28] Kosai Tanabe and Kazuko Sugawara Tanabe, Phys. Rev. C **95**, 064315, (2017).
[29] Kosai Tanabe and Kazuko Sugawara Tanabe, Phys. Rev. C **97**,069802 (2018).
[30] S. Frauendorf and F. Donau, Phys. Rev. C **89**,014322, (2014).
[31] S. Frauendorf, Phys. Rev. **C97**, 069801 (2018).
[32] R. Budaca, Phys. Rev. C **97**, 024302, (2018).
[33] J. T. Matta *et al.*, Phys. Rev. Lett. **114**, 082501 (2015).
[34] N. Senasharma *et al.*,Phys. Lett. B **792**, 170 (2019).
[35] Q. B. Chen, S. Frauendorf and C. M. Petrache, Phys. Rev. C **100**, 061301(R) (2019).
[36] J. Timar *et al.*, Phys. Rev. Lett. **122**, 062501 (2019).
[37] E. A. Lawrie, O, Shirinda and C. M. Petrache, Phys. Rev. C **101**, 034306 (2020).
[38] T. Holstein and H. Primakoff, Phys. Rev. **58**, 1098 (1940).
[39] T. F. Dyson, Phys. Rev. **102**,1217 (1958).
[40] V. Bargmann, Rev. Mod. Phys. **34**, 829(1962).
[41] J. Goldstone, Nuovo Cimento **19**, 154 (1961).
[42] A.S. Davydov and G.F. Filippov, Nucl. Phys. **8**, 788, (1958).
[43] L. Wilets and M. Jean, Phys. Rev. **102**, 788 (1956).
[44] J. Meyer-ter-Vehn, Nucl. Phys. **A249**, 111, 141, (1975).
[45] D. Bonatsos, D. Lenis, D. Petrellis and P. A. Terziev, Phys. Lett. **B 588** 172,(2004).
[46] D. Bonatsos, D. Lenis, D. Petrellis, P. A. Terziev and I. Yigitoglu, Phys. Lett. **B 621**, 102, (2005).
[47] A. A. Raduta, *et al.*, Nucl. Phys. **A 819**, 46 (2009).
[48] A.C. Davydov, *Teoria atomnova yadra*, Moscva, 1958 (in russian), chapters 19,20.
[49] H. Toki and Amand Faessler, Nucl. Phys. **A 253**, 231 (1975).
[50] H. Toki and Amand Faessler, Z. Physik **A 276**, 35 (1976).
[51] H. Toki and Amand Faessler, Phys. Lett. **B 63**, 121 (1976).
[52] H. Toki, K. Neergard, P. Vogel, and Amand Faessler, Nucl. Phys. **A 279**, 1 (1977).
[53] H. Toki, H. L. Yadav, A. Faessler, Phys. Lett. **B 66**, 310 (1977).
[54] T. Oguchi, Progr. Th. Phys, **25**,721 (1961).
[55] A. Gheorghe, A. A. Raduta, V. Ceausescu, Nucl. Phys. A 637, 201, (1998).
[56] M. E. Rose, *Elementary Theory of Angular Momentum* (Wiley, New York, 1957).
[57] D. Janssen, F. Donau, S. Frauendorf and R. V. Jolos, Nucl. Phys. **A 172**, 145 (1971).
[58] V. Ceausescu, A. A. Raduta, Prog. Th. Phys. **52** (3), 903 (1974)
[59] A.A.Raduta, A.Faessler and S.Stoica. Nucl.Phys.A 534, 149, (1991).
[60] A. Klein and E. R. Marshalek, Rev. Mod. Phys. **63**, 375 (1991).
[61] The convention of Rose [56] for the reduced matrix elements has been used